Transient Spectroscopy of Bacterial Rhodopsins with an Optical Multichannel Analyzer. 1. Comparison of the Photocycles of Bacteriorhodopsin and Halorhodopsin†

László Zimányi,‡ Lajos Keszthelyi,‡ and Janos K. Lanyi*
Department of Physiology and Biophysics, University of California, Irvine, California 92717
Received December 27, 1988; Revised Manuscript Received March 9, 1989

ABSTRACT: We used a gated optical multichannel analyzer to measure transient flash-induced absorption changes in bacteriorhodopsin (BR) and halorhodopsin (HR) and developed criteria for calculating the absorption spectra of the photocycle intermediates and the kinetics of their rise and decay. The results for BR agree with data reported by a large number of other authors. The results for HR in the presence of chloride are consistent with earlier data and reveal an additional intermediate, not previously seen, in the submicrosecond time scale. Although an M_{412}-like intermediate is not in the HR photocycle, a one-by-one comparison of the rest of the intermediates observed for BR and HR indicates a striking similarity between the photocycles of the two bacterial rhodopsins. This was previously not apparent, perhaps because the experimental approaches to the spectroscopy of the two pigments were different and the data were thus more fragmented.

Bacteriorhodopsin and halorhodopsin (BR and HR),[1] retinal proteins in the cytoplasmic membrane of halobacteria, function as light-driven pumps for protons and chloride ions, respectively [for reviews, see Stoeckenius et al. (1978), Stoeckenius and Bogomolni (1982), and Lanyi (1986a)]. Description of the photochemical reactions of these pigments is the first essential step in understanding the molecular processes which lead to the ion translocations. The photocycle and the photointermediates of BR have been studied extensively over almost 2 decades; studies of the HR photocycle are much more limited (Weber & Bogomolni, 1981; Tsuda et al., 1982; Schobert et al., 1983; Hazemoto et al., 1984; Steiner et al., 1984; Hegemann et al., 1985; Oesterhelt et al., 1985; Lanyi & Vodyanoy, 1986; Tittor et al., 1987).

The absorption of light by *all-trans*-BR is now understood to result in the initial photoproduct called J, which decays thermally on a picosecond scale to K, which in turn produces KL in <10 ns. KL decays to produce L_{550} over a few microseconds, and the latter produces M_{412}, where the Schiff base is deprotonated, in tens of microseconds. After M_{412}, all further transformations are on a similar (millisecond) time scale, and thus the intermediates of this time domain do not accumulate in observable amounts under all conditions. Nevertheless, current evidence favors a model (Kouyama et al., 1988; Fodor et al., 1988) in which reprotonation of M_{412} gives rise first to N, which produces O_{640} by reisomerization of the retinal, and the latter decays back to *all-trans*-BR. The intermediates are distinguished by their absorption spectra in the visible, red- or blue-shifted relative to the absorption of BR, as well as differences in their vibrational spectra which originate either from bond rotations or torsions in the retinal [e.g., see Smith et al. (1985)] or from changes in the protein [e.g., see Roepe et al. (1987) and Marrero and Rothschild (1987)].

The photoreaction of HR is not as thoroughly described. It is made more complex by the fact that different intermediates are produced in the presence and absence of chloride; i.e., the photocycle is influenced by whether the transported anion is provided or not. According to recent reports (Polland et al., 1985; Franz, 1988), in chloride-containing buffer the first intermediate, HR_K (or HR_{600}), is produced in the picosecond range, followed by the rise of HR_L (or HR_{520}) in about 1 μs (Tittor et al., 1987). HR_L decays, via a rather slow (several milliseconds) chloride-dependent equilibrium (Oesterhelt et al., 1985; Lanyi & Vodyanoy, 1986; Tittor et al., 1987), to HR_O (or HR_{640}), which regenerates HR_{578} within a few milliseconds. Since the chloride lost in the $HR_L \rightarrow HR_O$ step had to be regained, it was postulated (Oesterhelt et al., 1985) that the decay of HR_O generates first the chloride-free HR_{565}, known from spectroscopic titrations (Ogurusu et al., 1982; Taylor et al., 1983; Schobert et al., 1986), which then regains chloride in a step too rapid to allow observable accumulation of HR_{565}. In nitrate-containing buffer (i.e., in the absence of chloride), on the other hand, the initial photoproduct, which was reported to absorb also near 600 nm (Tittor et al., 1987; Franz, 1988), generates directly what was considered to be the same HR_O as in chloride (Lanyi & Vodyanoy, 1986; Tittor et al., 1987), which decays in a few milliseconds to regenerate HR_{565}.

The photoreactions of BR (and to a lesser extent HR) have been studied by a large number of different methods: measurement of transient flash-dependent absorption changes at single wavelengths, phase-modulation spectroscopy, measurement of photostationary states and their thermal transitions at low (e.g., liquid nitrogen) temperatures, photoacoustic spectroscopy, and, more recently, gated optical multichannel spectroscopy [references for the last method are Shichida et al. (1983), Milder and Kliger (1988), Dancshazy et al. (1988), and Tittor et al. (1987)]. Individually, many of these methods are deficient in one way or another: the sensitivity, the time and wavelength resolution, and the unambiguous interpretation

† This work was supported by a grant from the National Institutes of Health (GM 29498).
* To whom correspondence should be addressed.
‡ Permanent address: Institute of Biophysics, Biological Research Center of the Hungarian Academy of Sciences, Szeged, Hungary.

[1] Abbreviations: HR, halorhodopsin; BR, bacteriorhodopsin; HR_K (referred to elsewhere as HR_{600}), HR_{KL}, HR_L (elsewhere HR_{520}), and HR_O (elsewhere HR_{640}), photointermediates of HR, as described in the text; J, K, KL, L_{550}, M_{412}, O_{640}, and N, photointermediates of BR, according to general convention; Tris, tris(hydroxymethyl)aminomethane; MES, 2-(*N*-morpholino)ethanesulfonic acid.

0006-2960/89/0428-5165$01.50/0

of the results have presented problems. Thus, an ab initio solution of the photocycle (Nagle et al., 1982; Parodi et al., 1984) requires several kinds of measurements, and under various conditions. We feel, however, that once a photocycle model is at least tentatively accepted, optical multichannel spectroscopy can potentially supplant the other approaches for testing and refining it. The method has the significant advantage that it provides, from a single set of measurements, not only high-resolution ambient temperature spectra for the photointermediates which are otherwise difficult to obtain but also a set of rate constants for the entire reaction sequence. In spite of the large literature of BR, very few reports contain complete information of this kind for the photocycle under any given set of conditions. In our continuing exploration of the photoreactions of HR, and for a critical comparison of HR and BR, we use this method as a general way for determining the spectra and the kinetics of photointermediates under various experimental conditions. We anticipate that this measurement will be simple and rapid enough to be useful also in studying the effects of residue replacements (Khorana, 1988) in these pigments.

In this report, we show results with BR for calibration of the optical multichannel analyzer measurements and for arriving at criteria in the analyses of the data, and we describe the photocycle of HR in the presence of chloride. Using a single approach for examining the two pigments, as we do here, their photoreactions appear surprisingly similar to one another.

Materials and Methods

HR was purified from *Halobacterium halobium* strain OD-2W, using a newly described method (Duschl et al., 1988). The preparations were stored at 4 °C in 4 M NaCl, 25 mM Tris·HCl, pH 7.2, and 0.5% octyl glucoside, in the dark. Lubrol-solubilized HR was prepared by adding Lubrol PX (Pierce Chemicals, peroxide-free) to a final concentration of 0.5% and dialyzing 2–3 times against 100–200 volumes of a buffer containing 1 M NaCl/25 mM MES, pH 6.0, each time for approximately 12 h at 4 °C in the dark, in order to remove the octyl glucoside. Purple membrane was purified according to a published procedure (Oesterhelt & Stoeckenius, 1974). All measurements with purple membranes were in 25 mM Tris·HCl, pH 7.0.

Kinetic flash spectroscopy was carried out with a Princeton Instruments Corp. optical spectroscopic multichannel analyzer (OSMA) sketched in Figure 1A. The sample was placed in a 4 mm × 10 mm thermostated cuvette (the 4-mm path length in the direction of the measuring light) and was magnetically stirred. When the measurements were at 3 °C, condensation of moisture was prevented by blowing dry nitrogen on the cuvette faces. The actinic laser flash was at a right angle to the measuring light. The measuring light was polarized at the magic angle, taking into account the polarization ratio of the laser (Lozier, 1982), in order to eliminate possible effects of rotational diffusion of the particles on the kinetics. The measuring light (a white continuum) was provided by a 250-W OSRAM tungsten–halogen lamp operated at 173 W, and the incident intensity was effectively reduced by a 1.5-mm-diameter diaphragm placed immediately in front of the lamp to avoid actinic and heating effects. For the same reasons, the measuring light was chopped with a digital shutter (for the timing diagram, see Figure 1B). The actinic light source was a nitrogen laser pumped dye laser, of 600-ps pulse duration (Photochemical Research Associates Models LN 1000 and LN 102), where the tuning grating of the dye laser was replaced by a mirror for higher output power, and the wavelength maximum of the dye was 579 nm. After the sample, the

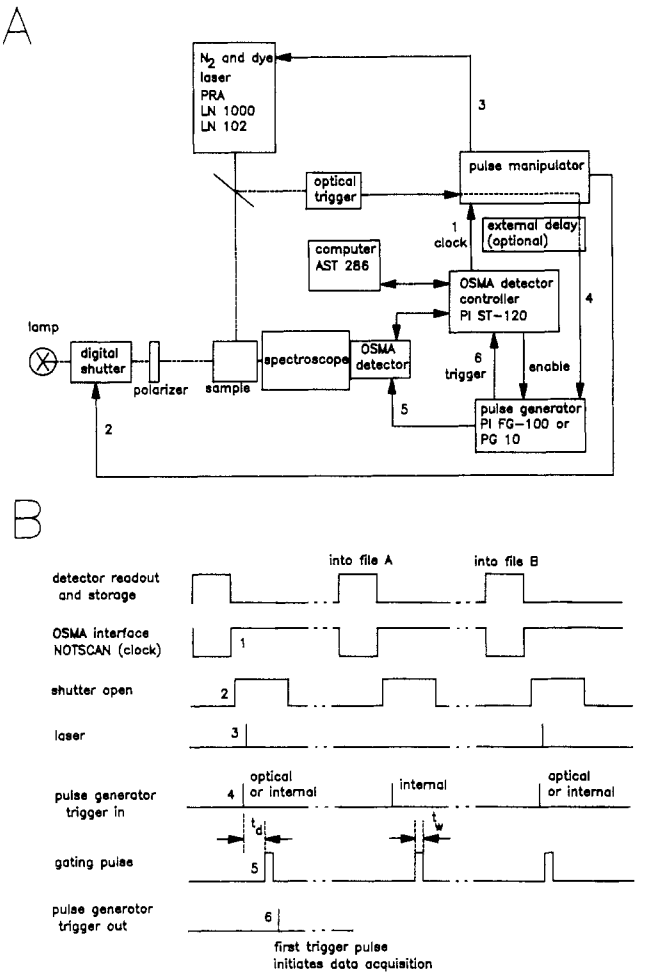

FIGURE 1: Description of the instrumentation used for optical multichannel analysis of absorbance transients. (A) Block diagram of the apparatus. The numbers 1–6 refer to timing signals in (B). (B) Timing diagram of the data acquisition control. Details are explained in the text.

measuring light was focused on the entrance slit of a Jarrell-Ash Monospec 27 spectroscope, equipped with a 150 groove/mm grating, blazed at 450 nm. The spectrum was projected onto a Princeton Instruments IRY-700S/B gated intensified diode array detector, connected to a Princeton Instruments ST-120 detector controller. Gating of the detector was with the Princeton Instruments FG-100 and PG-10 gate pulse generators, in the 50–250-ns and the 250 ns–7 ms delay ranges, respectively. Longer delays were generated externally with a Tektronix 535 A oscilloscope. The length of the gating pulses was varied from 20 ns to several microseconds, in order to provide optimal signal/noise ratios while keeping the pulses short relative to the delay times. The delay times given in the figures are the time intervals between the flash and the center of the gating pulse width. The control of data acquisition and analysis was with an AST 286 desktop computer, using software provided by Princeton Instruments Corp., as well as Lotus 123 spreadsheets. The timing of the experiments was set with a home-built TTL pulse manipulator.

The timing of trigger signals is shown in Figure 1B. The ST-120 detector controller ran freely with a frequency of several hertz, adjusted by software, providing an exposure time for the detector of several hundred milliseconds. The NOTSCAN output of the controller was used as primary clock pulse source (1). The pulse manipulator provided trigger pulses for the digital shutter (2), the laser (3), and the gate pulse generators (4). After the arrival of each NOTSCAN signal, the shutter was

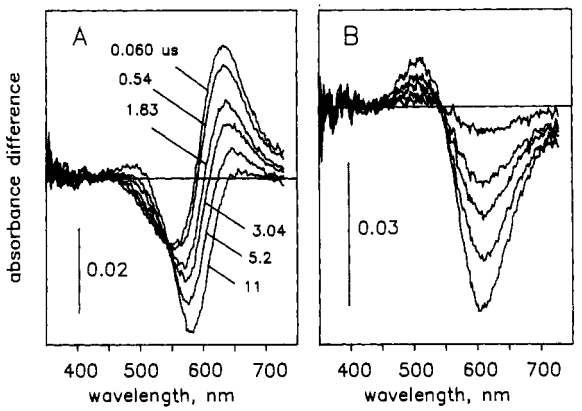

FIGURE 2: Flash-induced difference spectra of BR in the 60 ns–11 μs time domain, measured at 3 °C. The absorbance of the pigment at 570 nm was 0.4. (A) Measured difference spectra, at the delay times indicated. (B) Net difference spectra, constructed by subtraction of the 60-ns spectrum from each of the later spectra in (A). The BR transition seen is KL → L_{550} (cf. text).

opened for 20 ms (or 20–100 ms when longer delay times were selected). Five milliseconds after every second shutter opening, the laser was fired, and the signal from an optical trigger (Newport Corp.) was used to trigger the gate pulse generators. For every other shutter opening, when the laser was absent, a trigger pulse internally generated by the pulse manipulator was sent to the gate pulse generators. The gate pulse generators provided gating pulses of the desired delay and width (5), and the detector accumulated signals proportional to the light intensity at 700 out of the 1024 diodes during the gating, resolving the wavelength range of 307–725 nm. Readout and storage of the data followed each exposure period before the next acquisition cycle. The first trigger-out signal from the gate pulse generators (6) initiated the data acquisition sequence (ST-120 controller in the "external trigger" mode); after that, these trigger-out signals were disregarded by the detector controller. For each particular gating pulse delay, up to 1000 scans were averaged alternatingly into each of two separate files, one with and another without the laser. In this way, the ground-state absorption and the absorption of the intermediates were measured in parallel, eliminating the effect of slow changes in either lamp intensity or, more importantly, sample absorbance and scattering. As a result, the difference spectra calculated from the two files were virtually free of base-line distortions. The same cuvette with the corresponding buffer solution was used to record the incident light intensity, and using this, we calculated the absolute spectrum of the sample for each difference spectrum. When necessary, the difference spectra were normalized according to the absolute spectra, to eliminate effects of any changes in the sample absorbance over many measurements. A mathematically constructed light-scattering spectrum was subtracted for some of the absolute spectra, with the criterion that the resulting absorbance spectra closely resemble the absorbance of octyl glucoside solubilized HR, which is our most scatter-free preparation (Zimányi & Lanyi, 1987).

Results

Photocycle of BR. Difference spectra were measured for BR at increasing time delays after flash excitation; we give the results in the order of increasing time, grouped into time domains where transitions can be observed. Figure 2A shows representative traces at 3 °C for the earliest measured times, from 60 ns to 11 μs. Figure 2B contains the same difference spectra, but with the first trace subtracted so as to show the net absorbance changes during this time period. The single

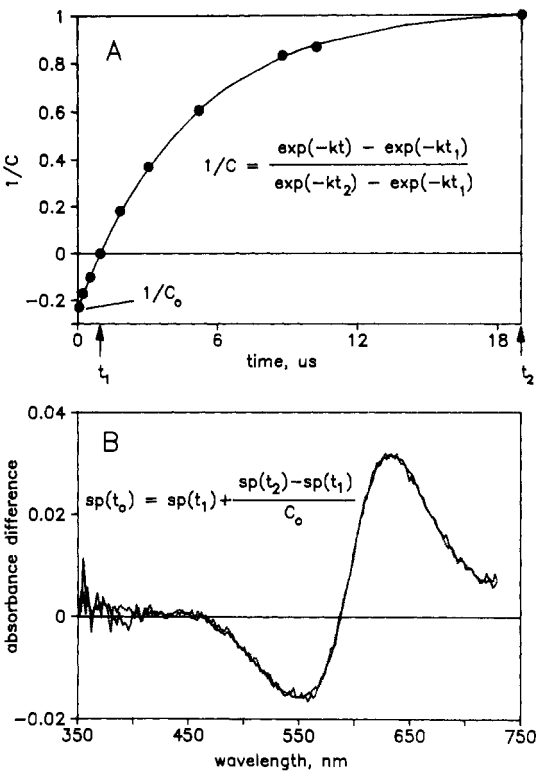

FIGURE 3: Extrapolation of the KL → L_{550} spectral transition in BR, shown in Figure 2, to zero time. (A) The expression in the figure, derived for a first-order reaction followed from $t = t_1$ to $t = t_2$ (1 and 19 μs, respectively), was used to extrapolate to zero time (—). C is the scaling factor for bringing net difference spectra between t and t_1 into agreement with that seen between t_2 and t_1 (●). The intercept of the line with the ordinate gives the correct scaling factor for predicting the zero time spectrum. (B) Comparison of the zero-time difference spectrum, predicted from difference spectra between 1 and 19 μs (···), and the measured 60-ns difference spectrum (—). The equation in the figure uses the scaling factor C_0, derived in (A), to predict a zero time (t_0) spectrum in which L_{550} has not yet formed, i.e., which consists purely of the difference between the spectra of KL and BR.

isosbestic points indicate that the process can be described by a single transition. The traces in Figure 2B suggest that this transition consists of depletion of a species which absorbs in the red and production of another species with absorbance in the green region, consistent with the KL → L_{550} step described for BR in this time domain (Shichida et al., 1983; Milder & Kliger, 1988). The actual absorbance maxima of these species will be given below.

Since the previous step, the K → KL process, is thought to take place between 1 and 10 ns at room temperature (Milder & Kliger, 1988), and possibly at longer times in our experiments at 3 °C, we examined the earliest traces for any contribution by the spectrum of K. This was done by extrapolating to zero time from those difference spectra for the KL → L_{550} transition which cannot contain K because they were collected much later, between 1 and 19 μs. The equations used assume a first-order transition, and are given in Figure 3A,B. We find that the time dependence of the amplitudes of the difference spectra can be fitted well with the line predicted by a single exponential (Figure 3A). The measured difference spectrum for 60 ns, furthermore, is virtually identical with the difference spectrum extrapolated from the 1–19-μs period to zero time (Figure 3B). The K intermediate is known to absorb near 610 nm (Schichida et al., 1983); i.e., it is significantly red-shifted from the spectrum of KL (see below) and would have distorted the 60-ns difference spectrum if present. Thus, the only intermediate we detect at 60 ns is KL.

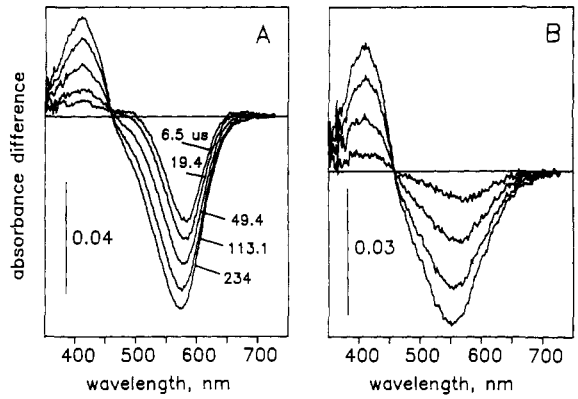

FIGURE 4: Flash-induced difference spectra of BR in the 6.5–234-μs time domain, measured at 22 °C. (A) Measured difference spectra, at the delay times indicated. (B) Net difference spectra, constructed by subtracting the 6.5-μs spectrum from each of the later spectra in (A). The transition seen is $L_{550} \rightarrow M_{412}$ (cf. text).

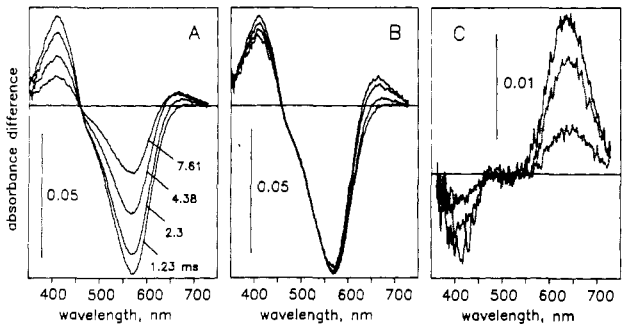

FIGURE 5: Flash-induced difference spectra of BR in the 1.23–7.61-ms time domain, measured at 22 °C. (A) Measured difference spectra, at the delay times indicated. (B) Scaled difference spectra, constructed by multiplying each of the spectra in (A) with an appropriate factor (cf. text), so as to eliminate the effect of the recovery of BR. (C) Net difference spectra, constructed by subtracting the 1.23-ms spectrum in (B) from each of the later spectra: 2.3 ms (- - -), 4.38 ms (···), and 7.61 ms (—). The transition seen is $M_{412} \rightarrow O_{640}$ (cf. text).

Subsequent spectra for the BR intermediates were taken at 22 °C, since the rates of rise and decay are such that O_{640} accumulates less at low temperatures (Gillbro, 1978). Figure 4 shows data for the time domain between 6.5 and 234 μs under these conditions. As before, Figure 4A contains measured difference spectra, while Figure 4B shows the same spectra with the first spectrum subtracted. The single isosbestic points in Figure 4A,B are again consistent with a single transition; from Figure 4B, it is identified as the $L_{550} \rightarrow M_{412}$ step.

The further transformations of the BR intermediates are more difficult to isolate, because subsequent steps overlap in time. In Figure 5, we show how the transitions can be identified in spite of this problem. Figure 5A contains measured difference spectra between 1.23 and 7.61 ms. The decrease of absorption in the blue region, reflecting the decay of M_{412}, is accompanied by an increase at both 570 nm (recovery of BR) and 650 nm (rise of O_{640}). The difference spectra were scaled to correct for the recovery of BR (Figure 5B). The appropriate scaling factors were derived by determining what fraction of the absolute spectrum of BR had to be added to the measured difference spectra in Figure 5A in order to obtain realistic absolute spectra for the M_{412} and O_{640} intermediates (see below). With the first scaled spectrum in Figure 5B subtracted from the others, the resulting net difference spectra (Figure 5C) clearly demonstrate the $M_{412} \rightarrow O_{640}$ transition and its kinetics over several milliseconds.

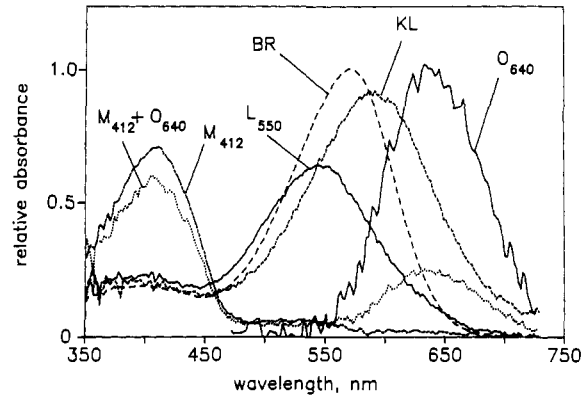

FIGURE 6: Calculated absolute spectra for the intermediates of the BR photocycle detected in Figures 2, 4, and 5. The method of calculation is described in the text. Extinctions are given relative to the extinction of light-adapted BR (also shown). Spectra of the individual species are labeled; since the spectrum of O_{640} was calculated from a mixture with M_{412}, the spectrum of this mixture is also given.

Figures 2, 4, and 5 contain difference spectra for all of the BR intermediates except J and K, which can be observed only at times well before 60 ns (Shichida et al., 1983; Milder & Kliger, 1988), and N, which does not accumulate under the conditions used (Kouyama et al., 1988). The absolute spectra of the BR intermediates detected were calculated from these figures. The method was analogous to what we used in reconstructing absolute spectra for HR photoproducts from low-temperature difference spectra (Zimányi & Lanyi, 1989). First, the fraction of BR which entered the photocycle was determined from difference spectra characteristic of the M_{412} intermediate, e.g., from that taken at 234-μs delay (Figure 4A). This photocycling fraction is the appropriate weighting factor used to multiply the absolute spectrum of BR, which is then added to the difference spectra to provide, after normalizing, a good absolute spectrum for the M_{412} intermediate. The photocycling fraction is easily obtainable for BR, because there is practically no overlap between the spectra of BR and M_{412}. The so-determined photocycling fraction was then used to reconstruct the absolute spectra of the corresponding intermediate mixtures from time zero up to about 1 ms, where still no detectable recovery of the parent species is observed. In the millisecond time domain, where the gradual recovery of BR becomes apparent, the criterion for finding the appropriate weighting factor, i.e., the remaining concentration of intermediates in the calculation of the absolute spectra, was that the absorbance between 470 and 540 nm be close to the base line, since M_{412} and O_{640} absorb minimally in this region. Figure 6 shows spectra for KL, L_{550}, M_{412}, an M_{412} *plus* O_{640} mixture, and for O_{640} calculated from the latter two. Because O_{640} does not accumulate in large amounts like the other species, its calculated spectrum is rather noisy. Nevertheless, it, as well as the other spectra, agrees with the maxima and shape of published spectra, obtained by a variety of methods, for the BR intermediates: in Figure 6, the maxima for KL, L_{550}, M_{412}, and O_{640} are at 590, 544, 410, and 640 nm, respectively. A survey of published room temperature spectra for these species indicates that their maxima are given at 596 and 543 nm (Shichida et al., 1983), 412 nm (Korenstein et al., 1978), and 640 nm (Lozier et al., 1975), respectively. In Figure 6, the extinctions of the four intermediates relative to that of BR are 0.87, 0.64, 0.71, and 1.02, respectively, while the published extinctions for room temperature spectra are 0.80 (Shichida et al., 1983), 0.66–0.73 (Shichida et al., 1983; Lozier et al., 1975), 0.72 (Nagle et al., 1982), and 0.79–0.92 (Lozier et al., 1975; Nagle et al., 1982), respectively.

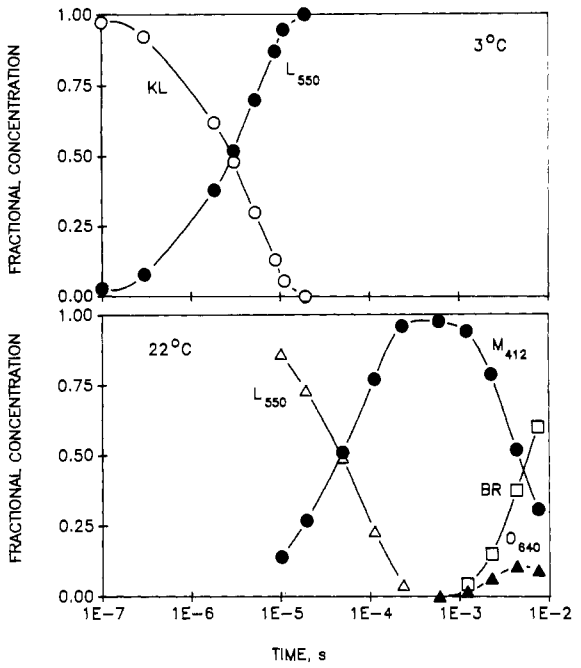

FIGURE 7: Kinetics of the transitions detected in Figures 2, 4, and 5. (Upper panel) Fractional concentrations for KL (○) and L_{550} (●) as functions of time after the flash, at 3 °C. (Lower panel) Fractional concentrations for L_{550} (△), M_{412} (●), O_{640} (▲), and BR (□) as functions of time after the flash, at 22 °C.

The difference spectra, such as in Figures 2–5, yield also the kinetics of the isolated transitions. Figure 7 shows the changes in the fractional concentrations of KL, L_{550}, M_{412}, O_{640}, and BR over a 5-decade time domain. The half-life for the KL → L_{550} transition at 3 °C is 2.8 μs, comparable to the reported 4.5 μs at 1 °C (Lozier et al., 1975). The half-lives of the rise and decay of M_{412} at room temperature are 48 μs, and 4.5 ms; some published results for these are 100 μs and 3–5 ms, respectively (Nagle et al., 1982). Kinetic modeling confirms that the shape of the transitions in Figure 7 corresponds to first-order reactions in time (not shown). The results for O_{640} in Figure 7 are consistent with an earlier kinetic study (Gillbro, 1978) where the maximal fractional concentration of this species, reached at 2.9 ms, was 0.23. The simplest explanation for the decreased accumulation of O_{640}, and its apparently delayed appearance relative to the recovery of BR, is that its decay rate constant is greater than its rise rate constant (Gillbro, 1978), unlike those of the other species detected here. Since the recovery of BR lags behind the decay of M_{412} (Figure 7), O_{640} can be placed between these two species in the photocycle.

Photocycle of HR. The photoreactions of HR in the presence of chloride were determined in a manner analogous to the measurements with BR. Figure 8 shows data at 3 °C for the earliest time domain, from 60 ns to 5.18 μs. The measured difference spectra in Figure 8A and the spectra with the first spectrum subtracted in Figure 8B contain single isosbestic points, consistent with a transition similar to that observed for BR in Figure 2. As with BR (Figure 3), extrapolation to zero time produced a single-exponential time course, and a difference spectrum for zero time indistinguishable from that measured at 60 ns (not shown). For reasons discussed below, we refer to the first intermediate detected in this way as HR_{KL}, and to the second as HR_L.

The next two transitions in the HR photocycle overlap in time, and the data were treated, accordingly, by the method shown for BR in Figure 5. The measured difference spectra at 22 °C in Figure 9A show more than one process: the

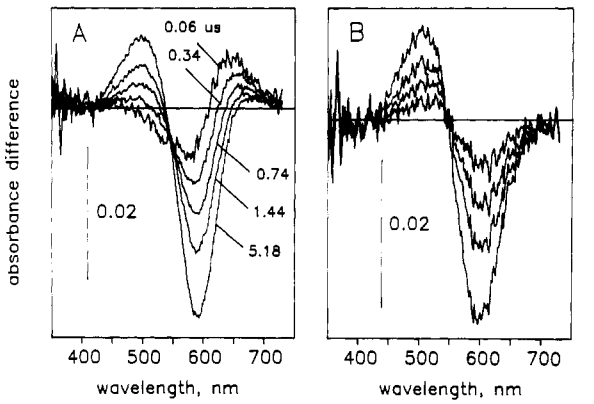

FIGURE 8: Flash-induced difference spectra of HR in the 60 ns–5.18 μs time domain, measured at 3 °C. The absorption of HR was 0.34. (A) Measured difference spectra, at the delay times indicated. (B) Net difference spectra, constructed from the spectra in (A) by subtracting the 60-ns spectrum from each of the later spectra. The transition seen is HR_{KL} → HR_L (cf. text.)

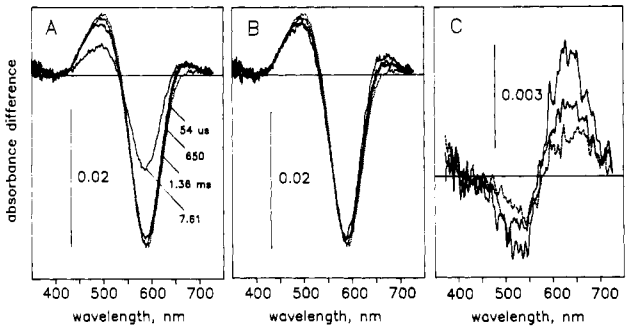

FIGURE 9: Flash-induced difference spectra of HR in the 54 μs–7.61 ms time domain, measured at 22 °C. The absorption of HR was 0.24. (A) Measured difference spectra, at the delay times indicated: 54 μs (···), 650 μs (- - -), 1.36 ms (-·-), 7.61 ms (—). (B) Scaled difference spectra, constructed by multiplying each of the spectra in (A) with an appropriate factor (cf. text), so as to eliminate the effect of the recovery of HR. (C) Net difference spectra, constructed by subtracting the 54-μs spectrum in (B) from each of the later spectra. The transition seen is HR_L → HR_O (cf. text).

decrease of absorption near 500 nm is accompanied, and on somewhat different time scales, by increases near both 590 nm and 660 nm. Scaled difference spectra are shown in Figure 9B; subtraction of the first of these from the others yielded the net difference spectra in Figure 9C. The latter indicate that during the recovery of HR, the decay of HR_L is connected to the small but distinct accumulation of a species which absorbs in the red (designated here as HR_O). This species was described earlier (Tittor et al., 1987) as HR_{640}. As shown in Figure 10, which contains data for the 3–22-ms time domain, events subsequent to the rise of HR_O do not affect the ratio of HR_L and HR_O but appear to consist of the simultaneous disappearance of these two species and the regeneration of HR. This is demonstrated by the fact that the difference spectra in Figure 10, normalized appropriately, are indistinguishable from each other within experimental error (not shown).

Figure 11 shows spectra for the detected intermediates of the HR photocycle, calculated following the same principles as in the case of BR. The photocycling fraction was determined from spectra in the tens of microseconds range, where there is virtually only a single intermediate present, i.e., HR_L. The criteria for accepting a calculated absolute spectrum were the same as in Zimányi and Lanyi (1989): the absorption of the putative intermediates should be nonnegative at all wavelengths, the wavelength dependence of the absorption should be smooth, each intermediate should have a single

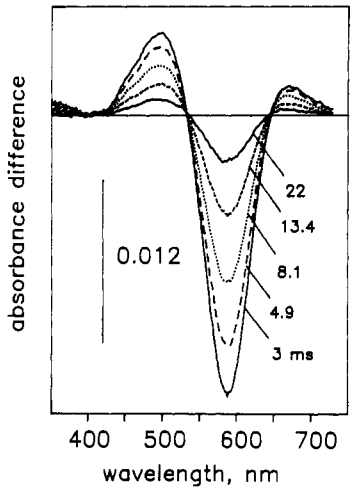

FIGURE 10: Flash-induced difference spectra of HR in the 3–22-ms time domain, measured at 22 °C. Measured difference spectra are shown, at the delay times indicated: 3 ms (—), 4.9 ms (– –), 8.1 ms (···), 13.4 ms (– · –), 22 ms (—).

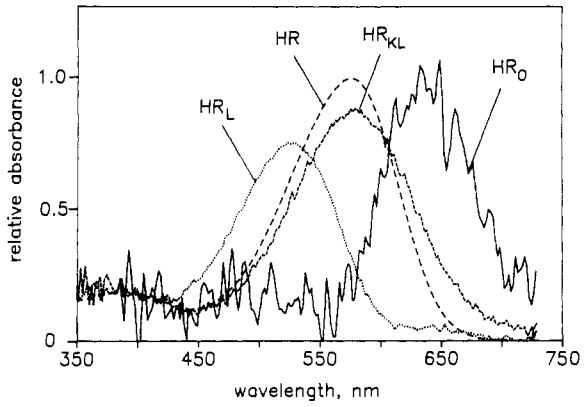

FIGURE 11: Calculated absolute spectra for the intermediates of the HR photocycle detected in Figures 8, 9, and 10. The method of calculation is described in the text. Extinctions are given relative to the extinction of light-adapted HR (also shown). Spectra of the individual species are labeled.

principal broad absorption maximum, and the characteristics (height, bandwidth, asymmetry) of the absorption bands should correspond to existing intermediate spectra in the literature for retinal proteins. In the millisecond region, the gradual recovery of the parent species was apparent from the distortion of the shape of the remaining HR_L spectrum when the same photocycling fraction was used as for earlier times. In this region, the actual concentrations of the decaying intermediates could be calculated by introducing decreasing photocycling fractions, which produced realistic absolute spectra for the HR_L and HR_O species. The weighting factors which yielded good absolute spectra for the HR_L *plus* HR_O mixtures in the millisecond time domain, and which provided the total concentration of the remaining intermediates, fitted a straight line in a logarithmic plot against time, as expected for the exponential recovery of HR at the end of the photocycle (not shown).

The spectra for HR_L and HR_O in Figure 11 agree approximately with spectra obtained earlier by flash spectroscopy (Tittor et al., 1987) and low-temperature spectroscopy (Zimányi & Lanyi, 1989) for HR_{520} and HR_{640}. However, consistent with that we observed before at lower temperatures, the absorption maximum of HR_L is at 526 nm rather than at 520 nm (Tittor et al., 1987). A second, small absorption band we always observe in the HR_L spectrum near 650 nm (Figure

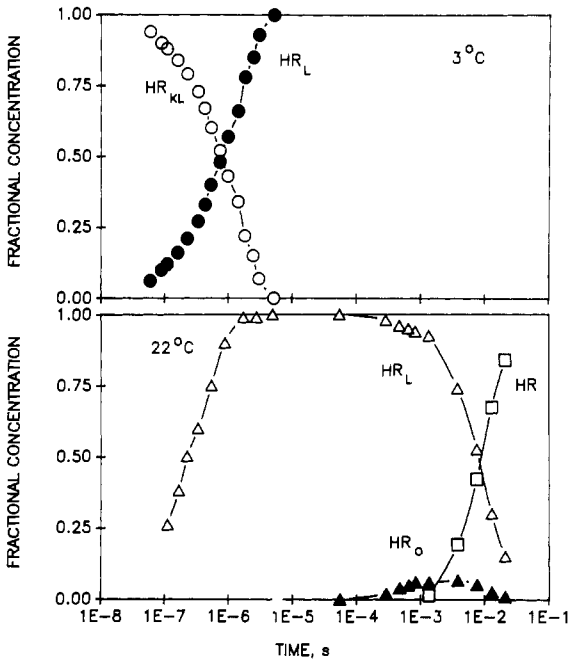

FIGURE 12: Kinetics of the transitions detected in Figures 8, 9, and 10. (Upper panel) Fractional concentrations for HR_{KL} (○) and HR_L (●) as functions of time after the flash, at 3 °C. (Lower panel) Fractional concentrations for HR_L (△), HR_O (▲), and HR (□) as functions of time after the flash, at 22 °C.

11) probably does not belong to HR_L, but to a red-shifted species of unknown origin, which arises on the same time scale as HR_L. The absorption maximum of HR_O, as determined here in the presence of 1 M chloride, is at about 638 nm. HR_{KL}, which absorbs at 578 nm, slightly red-shifted from the maximum of Lubrol-solubilized HR, and with a broader absorption band, has not been described before. The extinctions of HR_{KL}, HR_L, and HR_O in Figure 11, relative to that of HR, are 0.88, 0.76, and approximately 0.96, respectively. Earlier room temperature spectra for HR_L (in chloride) and HR_O (in nitrate) were both shown with relative extinctions of 0.79 (Tittor et al., 1987). A larger extinction for HR_O, relative to the HR_L, is supported by the shape of the $HR_L \rightarrow HR_O$ difference spectra (Figure 9C). In Figure 11, HR_{KL}, HR_L, and HR_O bear remarkable resemblance to the analogous BR intermediates (cf. Figure 6).

The kinetics of the HR photocycle are shown on a 7-decade time scale in Figure 12. The half-life of the $HR_{KL} \rightarrow HR_L$ transition at 3 °C is 0.8 μs; at room temperature, it is 0.23 μs. The half-life for the HR_L decay at room temperature is 8.2 ms. The absence of an M_{412}-like intermediate apparently results in the lengthened life time of the HR_L intermediate, as compared to the L species of the BR photocyle. Similarly to the O intermediate of the BR photocycle, HR_O rises and decays in the millisecond range, i.e., during the recovery of the parent pigment, and does not accumulate in large amounts. An additional similarity between these two red-shifted intermediates is that their transient concentration is even more decreased at lowered temperatures, e.g., at 3 °C (not shown). In fact, the production of HR_O from HR_L by a thermal transition is not at all observable at temperatures at or below 200 K (Zimányi & Lanyi, 1989). Unlike in the case of BR, however, the recovery of HR occurs with virtually the same rate as the decay of the previous intermediate, which is HR_L (Figure 12, lower panel). This is consistent with the fact that the ratio of HR_L and HR_O remains constant during the recovery of HR (cf. also Figure 10) and confirms the model (Oesterhelt et al., 1985; Tittor et al., 1987) in which an

equilibrium develops between HR_L and HR_O. The data do not decide, however, whether HR_O is an obligatory intermediate between HR_L and HR, i.e., between the linear model $HR_L \leftrightarrow HR_O \rightarrow HR$ and the branching model $HR_O \leftrightarrow HR_L \rightarrow HR$. The latter is ruled out by the fact that in that scheme the chloride dependency of the $HR_O \rightarrow HR_L$ step would cause decreased rates of decay for HR_O at lower chloride concentrations, and this, in fact, is not observed (Lanyi & Vodyanoy, 1986).

Discussion

Gated optical multichannel spectroscopy is a rapid and sensitive method for following the transient photoreactions of bacterial rhodopsins. With the exception of J and K, all of the intermediates of the BR photocycle which accumulate can be described, as regards their absorption spectra and the kinetics of their rise and decay. The results with BR (Figures 6 and 7) we obtain in this way agree well with previously reported information on the BR photocycle. Using the same method, we have described the HR photocycle in the presence of chloride (Figures 11 and 12). The results agree, in a general way, with previous data on HR (Oesterhelt et al., 1985; Lanyi & Vodyanoy, 1986; Tittor et al., 1987), but we found an additional intermediate, HR_{KL}. Although an M_{412}-like intermediate is not part of the HR photocycle, the rest of the species observed, and their kinetics, bear a striking resemblance to the intermediates of the BR photocycle. An analogy was drawn already between L_{550} and HR_L on the basis of their very similar resonance Raman spectra (Fodor et al., 1987). Because of these similarities, we adopt the designation for the HR species as simply HR with a subscript denoting their analogue in the BR photocycle.

In 1 M chloride, the spectroscopically detectable events of the HR photocycle consist of the following: $HR \rightarrow HR_K \rightarrow HR_{KL} \rightarrow HR_L \leftrightarrow HR_O \rightarrow HR$. We cannot detect HR_K at 60 ns or longer delay times; this intermediate is seen only at picoseconds (Polland et al., 1985) and in photoequilibria produced at 110 K (Zimányi & Lanyi, 1989). The HR species are defined by their absorption maxima, which are the following: HR_K at 598 nm (Tittor et al., 1987; Franz, 1988), HR_{KL} at 578 nm, HR_L at 526 nm, and HR_O at about 638 nm. Since light-adapted HR contains not only the all-trans but also some of the 13-cis isomeric form (Lanyi, 1986b), we expected a contribution from the photoreaction of the latter. From the results obtained, it is not clear what this contribution is; it might be the small amount of red-shifted species which is formed roughly at the same time as HR_L and is contained in the HR_L spectrum (Figure 11).

The spectroscopic similarity between the BR and HR intermediates does not necessarily imply that their molecular conformations are similar, any more than analogous photoproducts of visual rhodopsin and bacteriorhodopsin are similar. Although the retinal vibrational modes of HR_L (designated by these authors as hL) and L_{550} coincide even more than those of the parent species (Fodor et al., 1987), features of vibrational spectra which originate from protein residues in HR_L are more like those in M_{412} (Rothschild et al., 1988). Another difference is that the BR photocycle the reisomerization of retinal 13-cis to all-trans is in the $N \rightarrow O_{640}$ transition, but in the HR photocycle, it appears to be during the $HR_O \rightarrow HR$ step (Lanyi & Vodyanoy, 1986).

Until recently, BR and HR were the only retinal pigments known in halobacteria. As more and more bacterial rhodopsins are discovered (Spudich & Bogomolni, 1988; Mukohata et al., 1988), and mutated versions of these pigments are produced and studied (Khorana, 1988), the outlines of the structural and spectroscopic factors which unite this group of light-sensitive pigments will begin to emerge. The finding of substantial similarity between the photoreactions of BR and HR is a step in this direction.

Registry No. Cl^-, 16887-00-6.

References

Dancshazy, Zs., Govindjee, R., & Ebrey, T. G. (1988) *Proc. Natl. Acad. Sci. U.S.A. 85*, 6358–6361.

Duschl, A., McCloskey, M. A., & Lanyi, J. K. (1988) *J. Biol. Chem. 263*, 17016–17022.

Fodor, S. P., Bogomolni, R. A., & Mathies, R. A. (1987) *Biochemistry 26*, 6775–6778.

Fodor, S. P. A., Ames, J. B., Gebhard, R., van der Bergh, E. M. M., Stoeckenius, W., Lugtenburg, J., & Mathies, R. A. (1988) *Biochemistry 27*, 7097–7101.

Franz, A. (1988) Ph.D. Dissertation, Technical University, Munich, Federal Republic of Germany.

Gillbro, T. (1978) *Biochim. Biophys. Acta 504*, 175–186.

Hazemoto, N., Kamo, N., Kobatake, Y., Tsuda, M., & Terayama, Y. (1984) *Biophys. J. 45*, 1073–1077.

Hegemann, P., Oesterhelt, D., & Steiner, M. (1985) *EMBO J. 4*, 2347–2350.

Khorana, H. G. (1988) *J. Biol. Chem. 263*, 7439–7442.

Korenstein, R., Hess, B., & Kuschmitz, D. (1978) *FEBS Lett. 93*, 266–270.

Kouyama, T., Koyama, A. N., Ikegami, A., Mathew, M. K., & Stoeckenius, W. (1988) *Biochemistry 27*, 5855–5863.

Lanyi, J. K. (1986a) *Annu. Rev. Biophys. Biophys. Chem. 15*, 11–28.

Lanyi, J. K. (1986b) *J. Biol. Chem. 261*, 14025–14030.

Lanyi, J. K., & Vodyanoy, V. (1986) *Biochemistry 25*, 1465–1470.

Lozier, R. H. (1982) *Methods Enzymol. 88*, 133–162.

Lozier, R. H., Bogomolni, R. A., & Stoeckenius, W. (1975) *Biophys. J. 15*, 955–963.

Marrero, H., & Rothschild, K. J. (1987) *Biophys. J. 52*, 629–635.

Milder, S. J., & Kliger, D. S. (1988) *Biophys. J. 53*, 465–468.

Mukohata, Y., Sugiyama, Y., Ihara, K., & Yoshida, M. (1988) *Biochem. Biophys. Res. Commun. 151*, 1339–1345.

Nagle, J. F., Parodi, L. A., & Lozier, R. H. (1982) *Biophys. J. 38*, 161–174.

Oesterheld, D., & Stoeckenius, W. (1974) *Methods Enzymol. 31*, 667–678.

Oesterhelt, D., Hegemann, P., & Tittor, J. (1985) *EMBO J. 4*, 2351–2356.

Ogurusu, T., Maeda, A., Sasaki, N., & Yoshizawa, T. (1982) *Biochim. Biophys. Acta 682*, 446–451.

Parodi, L. A., Lozier, R. H., Bhattacharjee, S. M., & Nagle, J. F. (1984) *Photochem. Photobiol. 40*, 501–506.

Polland, H. J., Franz, M. A., Zinth, W., Kaiser, W., Hegemann, P., & Oesterhelt, D. (1985) *Biophys. J. 47*, 55–59.

Roepe, P., Ahl, P. L., Das Gupta, S. K., Herzfeld, J., & Rothschild, K. J. (1987) *Biochemistry 26*, 6696–6707.

Rothschild, K. J., Bousche, O., Braiman, M. S., Hasselbacher, C. A., & Spudich, J. L. (1988) *Biochemistry 27*, 2420–2424.

Schobert, B., Lanyi, J. K., & Cragoe, E. J., Jr. (1983) *J. Biol. Chem. 258*, 15158–15164.

Schobert, B., Lanyi, J. K., & Oesterhelt, D. (1986) *J. Biol. Chem. 261*, 2690–2696.

Shichida, Y., Matuoka, S., Hidaka, Y., & Yoshizawa, T. (1983) *Biochim. Biophys. Acta 723*, 240–246.

Smith, S. O., Lugtenburg, J., & Mathies, R. A. (1985) *J. Membr. Biol. 85*, 95–109.

Spudich, J. L., & Bogomolni, R. A. (1988) *Annu. Rev. Biophys. Biophys. Chem. 17*, 193–215.
Steiner, M., Oesterhelt, D., Ariki, M., & Lanyi, J. K. (1984) *J. Biol. Chem. 259*, 2179–2184.
Stoeckenius, W., & Bogomolni, R. A. (1982) *Annu. Rev. Biochem. 51*, 587–616.
Stoeckenius, W., Lozier, R. H., & Bogomolni, R. A. (1978) *Biochim. Biophys. Acta 505*, 215–278.
Taylor, M. E., Bogomolni, R. A., & Weber, H. J. (1983) *Proc. Natl. Acad. Sci. U.S.A. 80*, 6172–6176.
Tittor, J., Oesterhelt, D., Maurer, R., Desel, H., & Uhl, R. (1987) *Biophys. J. 52*, 999–1006.
Tsuda, M., Hazemoto, N., Kondo, M., Kamo, N., Kobatake, Y., & Terayama, Y. (1982) *Biochem. Biophys. Res. Commun. 108*, 970–976.
Weber, H. J., & Bogomolni, R. A. (1981) *Photochem. Photobiol. 33*, 601–608.
Zimányi, L., & Lanyi, J. K. (1987) *Biophys. J. 52*, 1007–1013.
Zimányi, L., & Lanyi, J. K. (1989) *Biochemistry 28*, 1662–1666.

Transient Spectroscopy of Bacterial Rhodopsins with an Optical Multichannel Analyzer. 2. Effects of Anions on the Halorhodopsin Photocycle†

László Zimányi‡ and Janos K. Lanyi*
Department of Physiology and Biophysics, University of California, Irvine, California 92717
Received December 27, 1988; Revised Manuscript Received March 9, 1989

ABSTRACT: We find that the photocycle of halorhodopsin (HR) in the presence of nitrate (but not chloride) consists of two parallel series of reactions. The first is essentially the same as that which occurs in the presence of chloride: $HR \xrightarrow{h\nu} HR_K \rightarrow HR_{KL} \rightarrow HR_L \leftrightarrow HR_O \rightarrow HR$. The second photocycle, however, which we describe as $HR \xrightarrow{h\nu} HR'_K \rightarrow HR_{KO} \rightarrow HR_O \rightarrow HR$, seems characteristic of what one would observe in the absence of chloride. Absorption spectra are calculated for all species but HR_K and HR'_K, which occur at shorter times (<60 ns) than we can resolve. At nitrate concentrations between 0.1 and 1 M, the proportion of HR which enters the first kind of photocycle increases in such a way as to suggest that nitrate can substitute for chloride, but much less effectively. At lower anion concentrations, the two photocycles are independent of one another, but at higher concentrations, they interact; i.e., the reaction $HR_{KO} \rightarrow HR_O \rightarrow HR_L$ can be observed. Thus, HR_O must be common to the two photocycles. Kinetic fitting of the time dependence of HR_L and HR_O at different chloride concentrations provides evidence for the participation of chloride in the interconversion of HR_L and HR_O. The results are consistent with a model in which the photoreaction is influenced by the binding of an anion (either chloride or nitrate) to site II in HR: when an anion is bound, the HR_K-initiated HR_L-type photocyle is observed, but when the site is not occupied, the HR'_K-initiated HR_O-type photocycle is seen.

Halorhodopsin (HR),[1] a retinal protein in the cytoplasmic membrane of extremely halophilic bacteria (Lanyi, 1986), is a light-driven pump for chloride ions. In the presence of chloride, absorption of light by the *all-trans*-retinal-containing chromophore of this pigment generates a transient bathochromic photoproduct (Polland et al., 1985; Franz, 1988), similar to the K intermediate of BR (Becher et al., 1978; Iwasa et al., 1980; Shichida et al., 1983). Relaxation back to HR is over several milliseconds; the ensuing sequence of thermally driven reactions (photocycle) should be regarded as the reaction cycle which drives chloride across the membrane. There is evidence with detergent-solubilized HR (Polland et al., 1985; Oesterhelt et al., 1985; Lanyi & Vodyanoy, 1986; Tittor et al., 1987; Zimányi et al., 1989) that the photocycle in the presence of chloride includes the following reactions:

$$HR{\cdot}Cl^- \xrightarrow{h\nu} HR_K{\cdot}Cl^- \rightarrow HR_{KL}{\cdot}Cl^- \rightarrow HR_L{\cdot}Cl^- \leftrightarrow HR_O \rightarrow HR \leftrightarrow HR{\cdot}Cl^-$$

The intermediates in this scheme are very similar (Zimányi et al., 1989) to those in the photocycle of BR; the most conspicuous difference between the two pigments is that in HR a deprotonated intermediate is not part of the reaction sequence (Hegemann et al., 1985). For the translocation of chloride, the critical step may be the reversible equilibrium of $HR_L{\cdot}Cl^-$ with HR_O (Oesterhelt et al., 1985), driven in favor of chloride release by the subsequent step, $HR_O \rightarrow HR$, which must represent the (irreversible) reisomerization of the retinal. Although evidence for this is still lacking, it seems likely that the chloride released at this step is the transported chloride. The $HR \leftrightarrow HR{\cdot}Cl^-$ equilibrium has been described before on the basis of a small red-shift in the absorption maximum of HR, which accompanies the binding of chloride to the so-called site II in the protein (Schobert et al., 1986). Under physiological conditions (i.e., high NaCl concentrations), this equilibrium is driven far in favor of chloride uptake, and it is assumed to occur in the photocycle, as written above, in order

† This work was supported by a grant form the National Institutes of Health (GM 29498).
* To whom correspondence should be addressed.
‡ Permanent address: Institute of Biophysics, Biological Research Center of the Hungarian Academy of Sciences, Szeged, Hungary.

[1] Abbreviations: HR, halorhodopsin; BR, bacteriorhodopsin; HR_K (referred to elsewhere as HR_{600}), HR'_K (elsewhere HR_{600}), HR_{KO}, HR_{KL}, HR_L (elsewhere HR_{520}), and HR_O (elsewhere HR_{640}), photointermediates of HR, as described in the text; MES, 2-(*N*-morpholino)ethanesulfonic acid.

0006-2960/89/0428-5172$01.50/0